Proceedings of the 2011 IEEE
International Conference on Robotics and Biomimetics
December 7-11, 2011, Phuket, Thailand

ORF-MOSAIC for Adaptive Control of a Biomimetic Arm

M. Mahdi Ghazaei A. and Henrik Jörntell and Rolf Johansson

Abstract— **This study is an attempt to take advantage of a *cerebellar model* to control a *biomimetic arm*. The cerebellar controller is a modified MOSAIC model which adaptively controls the arm. We call this model ORF-MOSAIC (*Organized by Receptive Fields* MOdular Selection And Identification for Control). The arm features a musculoskeletal model which is controlled through muscle activations by means of optimization techniques. With as few as 16 modules, we were able to control the arm in a workspace of 30×30 cm. The system was able to adapt to an external field as well as handling new objects despite delays. The discussion section suggests that there are similarities between the microzones in the cerebellum and the modules of this new model.**

I. INTRODUCTION

As robotic technology moves toward more anthropomorphic structures with increased complexity, it is reasonable to consider controllers inspired by human anatomy too. Although the robotics technology has achieved great performance in terms of accuracy, speed and robustness, the results are still limited to well-defined tasks. On the other hand, biological systems can operate under variety of conditions and their flexibility is yet unrivaled.

One of the features of motor control in the vertebrates is fast-reaching movements in spite of long delays and noise in the nervous systems. It is believed that the cerebellum is mainly responsible to compensate for such deficiencies.

In the attempt to explain the functionality of the cerebellum, several computational models ranging from the cellular level to the functional level have been developed. The following list summarizes the major computational models:

1) Cerebellar Model Articulation Controller (CMAC) [1];
2) Adjustable Pattern Generator (APG) [2];
3) Schweighofer-Arbib [3];
4) Cerebellar feedback-error-learning model (CBFELM) [4];
5) Multiple paired forward-inverse model (MPFIM) [5].

The last model which was later on renamed Modular Selection and Identification for Control (MOSAIC) [6] is a high-level functional model. It aims to describe different behavioral observations such as context dependent control or generalization to new tasks.

This research was supported by the Linnaeus Center LCCC, Swedish Research Council; Ref. VR 2007-8646

M. M. Ghazaei Ardakani is with the Department of Computer Science, Faculty of Engineering, Lund University, 221 00 Lund, Sweden Email: mahdi.ghazaei@cs.lth.se, mghazaei@gmail.com

H. Jörntell is with the Department of Experimental Medical Sciences, Section for Neurophysiology, Lund University, The Biomedical Center F10, 221 84 Lund, Sweden Email: henrik.jorntell@med.lu.se

R. Johansson is with the Department of Automatic Control, Faculty of Engineering, Lund University, 221 00 Lund, Sweden Email: rolf.johansson@control.lth.se

There are a few fundamental assumptions in this model. Most importantly, similar to CBFELM it advocates internal model hypothesis which states that the cerebellum realizes an internal model of the body parts in order to successfully control them [7]. The structure of MOSAIC hosts both forward models and inverse models paired in modules.

Modularity is thought to be another important feature of the motor control [8], in particular the cerebellum [9], [10]. A high degree of flexibility without overly complicated control and adaptation mechanisms is possible through a modular approach. Thereby, the key to success is an efficient way to combine the modules. In MOSAIC model, the responsibility signals derived from the contextual information and the predictions of the forward models adjust the contributions of the corresponding inverse models.

Since the original paper on MOSAIC [5], there have been some development in its application and a few extensions. There is a successful report on the application of the original proposal for controlling three different objects, characterized by mass, weight, and damping factor. In this report, the system was able to learn multiple tasks (controlling an object), generalize to a new task and switch between tasks appropriately [11].

HMM-MOSAIC [6], is a variant which make use of Hidden Markov Model (HMM) for improving both the training and the switching aspects of MOSAIC. The methodology is inspired by speech processing techniques and the training algorithm is a specialized instance of Expectation Maximization (EM) algorithm. Though it is difficult to motivate this probabilistic approach biologically, it is argued by the authors that the context estimation by human could be well described by HMM models.

The same authors extended their model later to a hierarchical MOSAIC, ***HMOSAIC*** [12]. In this paradigm, the modules could be cascaded. A higher-level MOSAIC receives an abstract desired trajectory and posterior probabilities of its subordinate level and generates as a motor command, prior probabilities for the lower-level modules. The model was tested with the same three objects.

In [13], ***e-MOSAIC*** was proposed and used for humanoid robot control. In this architecture, forward models serve as state estimators in form of Kalman filters and contribute to the overall state estimate. Instead of inverse models, for each observer a matching Linear Quadratic (LQ) controller is designed which together with the overall state estimate, functions as a Linear Quadratic Gaussian (LQG) controller. The responsibility weighted summation of these LQG controllers constitute the control signal. The models are fixed with no adaptation.

978-1-4577-2138-0/11/$26.00 © 2011 IEEE

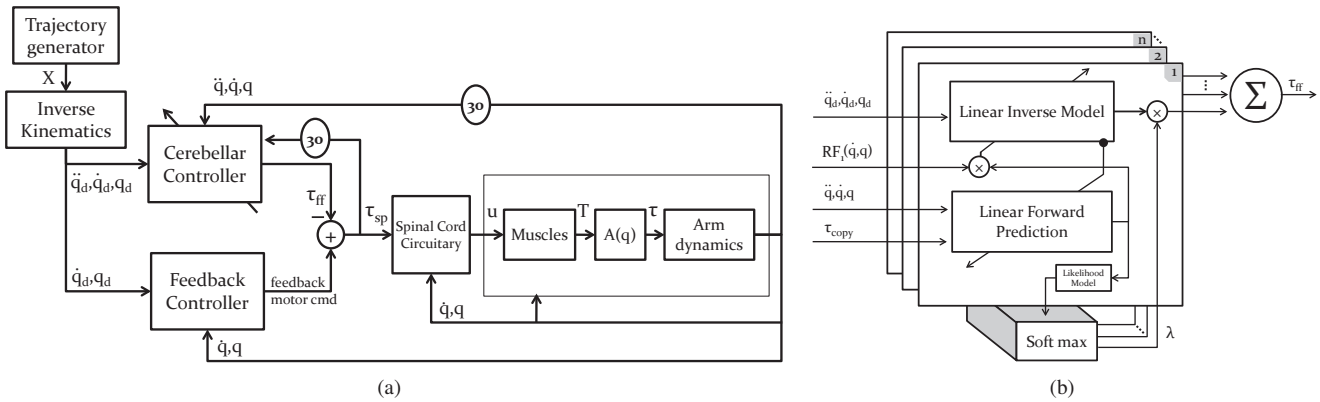

Fig. 1. (a) A high-level structure of the complete control loop; (b) ORF-MOSAIC structure, $\mathrm{RF}_n(\dot{q},q)$ indicates receptive field function, q_d desired trajectory, q feedback signals, τ_{copy} efference copy, λ responsibility signal. The forward prediction block is paired to the inverse model and uses the same parameters.

MOSAIC scheme has also been extended to the reinforcement learning paradigm as multiple model-based reinforcement learning (***MMRL***), in which each inverse model controller was replaced by a reinforcement learning agent [14]. The authors have developed discrete and continuous cases in parallel and tested the structure in a haunting task in a grid world and for controlling an inverted pendulum.

In order to control sit-to-stand task, an automatic module assigning MOSAIC, ***AMA-MOSAICI*** was proposed in [15]. The whole task is decomposed to linear subtasks by a clustering algorithm. The main feature of this work is that the number of the required modules is automatically determined. However, both clustering and training are done off-line.

II. PROBLEM STATEMENT

According to the review, so far either the application of MOSAIC model has been limited to simple problems or major modifications to the model were required. Initially, the MOSAIC model is a functional model and not a biological one. However, it has been even further moved away from its biological roots toward more classic control or reinforcement learning approaches for more serious applications. In these applications, adaptation is limited if exists at all and no attention has been paid to delays.

This article presents ORF-MOSAIC (**Organized by Receptive Fields** MOdular Selection And Identification for Control) as a biologically inspired cerebellar model to adaptively control a human-like robotic arm with potential delays.

A. Assumptions

Here, the assumptions for our models are summarized. Similar assumptions are commonly made and they are partly supported by biological evidences.

- The motor cortex is responsible for trajectory planning in the form of minimum jerk [16];
- Planning is done in task space, control in joint space and there is a transformation to muscle space [17] (for joint based control see [18]);
- The cerebellum builds internal models so that after learning control is done by inverse models [19];
- The sensory system through either proprioceptive or cutaneous receptors is able to provide an estimate of joint angles, angular velocity and acceleration [20], [21];
- Muscle coactivation works in a way that in an agile motion the total tension across muscles is minimized.

Fig. 1(a) shows the block diagram of the complete plant. It highlights the building blocks and the assumed variables.

The assumption about the coordinate transformations makes it possible to divide the problem into two fairly independent subproblems. Therefore, as the first stage, we realized a *Minimum Tension Control* algorithm which takes care of the transformation between the joint space to the muscle space. Several trajectories within a reasonable range of speeds for a human arm were experimented. It turned out that the algorithm is able to produce a near perfect transformation from the required torques to the activation signals in the given range. Therefore, in this paper we direct our attention toward the development of ORF-MOSAIC and save those details for an appropriate place.

III. MODEL OF ARM

The dynamics of a human arm could be analyzed similarly to solid multi-joint manipulators. In that case, the equations of motion are usually derived by the Lagrange's equations. These equations have a generic form of:

$$M(q)\ddot{q}+C(q,\dot{q})+E(q,\dot{q})+G(q)=\tau, \qquad (1)$$

where $M(q)$ is a symmetric positive definite inertia matrix, $C(q,\dot{q})$ is the vector of centripetal and Coriolis torques, $E(q,\dot{q})$ is the effect of an external force field and $G(q)$ is the term due to gravity. $q\in\mathbb{R}^n$ is the vector of joint angels and its time derivatives denoted by dot operator. The system is driven by torque vector, $\tau\in\mathbb{R}^n$.

For the sake of simplicity, a two link model according to Fig. 2 can represent the human arm. If we further limit the motion in a horizontal plane, only two joints with one degree of freedom are required and the effect of gravity is ignored.

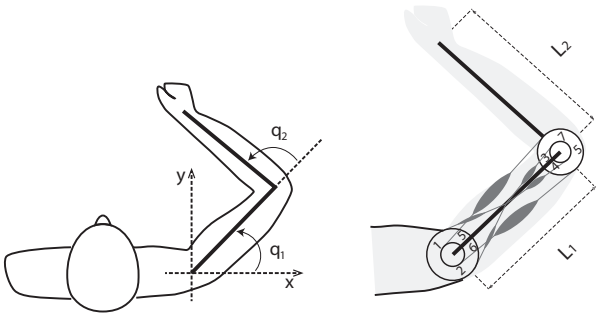

Fig. 2. Schematic of Arm and its geometry

In this case, the matrices in (1) are as follows:

$$M(q) = \begin{pmatrix} a_1 + 2a_3\cos(q_2) + a_2 & a_3\cos(q_2) + a_2 \\ a_3\cos(q_2) + a_2 & a_2 \end{pmatrix} \quad (2)$$

$$C(\dot{q}, q) = \begin{pmatrix} -a_3\sin(q_2)\dot{q}_2 & -a_3\sin(q_2)(\dot{q}_1 + \dot{q}_2) \\ a_3\sin(q_2)\dot{q}_1 & 0 \end{pmatrix} \dot{q} \quad (3)$$

$$a_1 = m_2 L_1^2 + m_1 r_1^2 + I_1 \quad (4)$$

$$a_2 = m_2 r_2^2 + I_2 \quad (5)$$

$$a_3 = m_2 L_1 r_2 \quad (6)$$

where the subscripts of q indicate its elements; with indices denoting the link number, m, L, r, and , I refer to link mass, link length, the distance between the previous joint to the center of the gravity of a link, and moment of inertia around the center of mass, respectively. These values for an average male person could be chosen according to Table I [22].

TABLE I

GEOMETRICAL AND DYNAMICAL PARAMETERS OF THE ARM

	m (kg)	L (m)	r (m)	I (kg.m^2)
Link 1	1.59	0.3	0.13	0.0216
Link 2	1.44	0.35	0.14	0.0089

Another aspect of a human arm is its musculoskeletal structure, i.e., how muscles are connected to the bones. With an eye on robotic application, a model according to Fig. 2 could be devised. This model [23] has the feature of both *mono-articular* and *bi-articular* muscles and with right parameters can closely simulate a human arm. Following [23], we used a constant moment arm matrix and a Hill-type muscle model.

IV. ORF-MOSAIC

Fig. 1(b) shows the architecture of this model. Similarly to MOSAIC, the control signal is generated by inverse models. An inverse model receives the desired output and produces the right command to achieve that. Furthermore, each inverse model (consequently a module) shares a portion of the responsibility in controlling a plant based on the quality of the prediction of its forward model. The forward models which have access to the sensory feedback and the efference copy, predict the consequences of a motor command.

The inverse and forward models can be mathematically formulated as follows:

$$u_i(t) = \psi(w_i(t), x^*(t)) \quad (7)$$

$$u_{ff}(t) = \sum_{i=1}^{n} \lambda_i(t) u_i(t) \quad (8)$$

$$\hat{\dot{x}}_i(t) = \phi\left(w_i(t), x(t-d), u(t')\right) \quad (9)$$

$$\hat{\dot{x}}(t) = \sum_{i=1}^{n} \lambda_i(t) \hat{\dot{x}}_i(t), \quad (10)$$

where x^*, $x(t-d)$, and $\hat{\dot{x}}_i$ are the desired state, delayed sensory feedback, and the output of i-th forward model, respectively. Here, u_i represents i-th module's control signal, u_{ff} total feedforward control signal, and $u(t')$ the efference copy containing the history of u between $(t-d, t]$, $\psi(\cdot)$ and $\phi(\cdot)$ being inverse and forward functions, respectively. In the continuous case, we have considered the time derivative of the state as the prediction of forward models. Also, forward models are literally paired to the inverse models so that they share the same vector of parameters, w_i.

Assuming a Gaussian posterior probability and a prior probability P_i, the responsibility signal, $\lambda_i(t)$ is calculated according to the Bayes' theorem.

For training such a network, two questions must be confronted; which module and when it must be trained. These are formally known as *structural* and *temporal credit assignment*. To tackle the first problem, we have introduced the receptive field concept. Each module according to (11) has a signature receptive field modulating its training and giving rise to the organizational structure of the modules.

$$\mu_i(t) = RF_i(x(t)) = e^{-(x(t)-x_i)^T \Sigma_i (x(t)-x_i)}, \quad (11)$$

is a radial base function with the highest reception at $x(t) = x_i$ and Σ_i determines the shape of the receptive field.

This implies that unlike MOSAIC, we have dissociated control from learning. In other words, the same responsibility signal does not determine which module is adapting. The second problem is addressed by time alignment of regressors and adjustment signals.

Given the above mentioned assumptions, a gradient descent type of learning can be formulated as below:

$$\Delta w_i(t) = \gamma RF_i(x(t-d)) \frac{d\psi_i}{dw_i} \left(u^*(t-d) - u_i(t-d)\right) \quad (12)$$

$$\simeq \gamma \mu_i(t-d) \frac{d\psi_i}{dw_i} \chi\left(\dot{x}(t-d) - \hat{\dot{x}}_i(t-d)\right), \quad (13)$$

where γ is the learning rate. Apparently, the standard of correctness is not available in the coordinate system of u. To overcome the distal error problem, function χ should provide an approximation by transforming the error of the forward prediction.

A. Implementation

1) Inverse Models: Equation (1) is possible to be rewritten in a linear form with respect to unknown parameters such that

$$\tau = \Psi(q, \dot{q}, \ddot{q})\theta, \quad (14)$$

where θ is a row vector containing the unknown parameters and Ψ is the regressor.

We consider an external field of the following form:

$$E = B\dot{q} = \begin{pmatrix} b_1 & b_2 \\ b_3 & b_4 \end{pmatrix} \dot{q}, \tag{15}$$

where $\dot{q}$ is the angular velocity vector, and B is a constant matrix representing viscosity of the environment in the joint space.

Consequently, if we use the notation of $c_2 = \cos(q_2)$ and $s_2 = \sin(q_2)$, together with the parameters of Sec. III, it is easily shown that

$$\theta = (a_1, a_2, a_3, b_1, b_2, b_3, b_4)^T, \tag{16}$$

$$\Psi(q,\dot{q},\ddot{q}) = \begin{pmatrix} \psi_{11} & \psi_{12} & \psi_{13} & \psi_{14} & \psi_{15} & 0 & 0 \\ 0 & \psi_{22} & \psi_{23} & 0 & 0 & \psi_{26} & \psi_{27} \end{pmatrix} \tag{17}$$

$$\begin{aligned} \psi_{11} &= \ddot{q}_1, \ \psi_{12} = \ddot{q}_1 + \ddot{q}_2 \\ \psi_{13} &= 2\ddot{q}_1 c_2 + \ddot{q}_2 c_2 - 2\dot{q}_1\dot{q}_2 s_2 - \dot{q}_2^2 s_2 \\ \psi_{14} &= \dot{q}_1, \ \psi_{15} = \dot{q}_2 \\ \psi_{22} &= \ddot{q}_1 + \ddot{q}_2, \ \psi_{23} = \ddot{q}_1 c_2 + \dot{q}_1^2 s_2 \\ \psi_{26} &= \dot{q}_1, \ \psi_{27} = \dot{q}_2. \end{aligned}$$

We are interested in linear inverse models such that

$$\hat{\tau} = \hat{\Psi}(q_d, \dot{q}_d, \ddot{q}_d)\theta \tag{18}$$

$$\hat{\Psi}(q,\dot{q},\ddot{q}) = \ddot{Q}^T A + \dot{Q}^T B + Q^T C + D, \tag{19}$$

where $A, B, C \in \mathbb{R}^{n^2 \times p}$ and $D \in \mathbb{R}^{n \times p}$. The number of joints is denoted by n and p is the length of θ. $Q \in \mathbb{R}^{n^2 \times n}$ is a matrix where vector q could be thought as its diagonal elements.

Equation (19) in the component form equals to

$$\hat{\psi}_{ij} = A_{ij}^T \ddot{q} + B_{ij}^T \dot{q} + C_{ij}^T q + D_{ij}, \tag{20}$$

where coefficient vectors are 2×1 and D_{ij} is scaler in our problem.

An easy way to obtain such representation is through considering an operating point and linearizing (17) around that point (i.e., by 1st-order Taylor series expansion). Moreover, such an operating point correspond to x_i in (11). Although this is not the only approach but it offers an easy way to formulate an inverse model which preserves the same parameters as in (16)[1].

Note that the derivative of ψ_i in (13) with respect to the vector of the parameters is simply $\hat{\Psi}(q_d, \dot{q}_d, \ddot{q}_d)$.

2) Forward Models: By examining (1) closely, we see that substituting $\ddot{q}$ with $-H^{-1}(q)\tau$ and τ with $-M(q)\ddot{q}$ does not change the equation. We can use this property to reuse (18) for forward models. Therefore, we define

$$\hat{\ddot{q}} = -\hat{M}^{-1}\hat{\Psi}(q,\dot{q},-\hat{M}^{-1}\tau)\theta. \tag{21}$$

Collecting terms with $\ddot{q}$ from (17) leads us to $M(q)$. It is possible to collect terms in the same way from (18) irrespective of how we have obtained the linear equations. The resulting matrix defines $\hat{M}$ which is no longer a function of q but a constant function linear in the parameters.

3) Distal Error Transformation: Here we suggest a function $\chi(e(t)) = -\hat{M}e(t)$ matched with the forward and the inverse models of a module for such transformation.

To motivate this, consider the error in the prediction of a forward model. If we substitute $\hat{\ddot{q}}$ from (21), we obtain:

$$\ddot{q} - \hat{\ddot{q}} = \ddot{q} + \hat{M}^{-1}\hat{\Psi}\left(q,\dot{q},-\hat{M}^{-1}\tau\right)\theta \tag{22}$$

Now, we multiply both sides of the equation by $-\hat{M}$ to derive,

$$\begin{aligned} -\hat{M}(\ddot{q} - \hat{\ddot{q}}) &= -\hat{\Psi}\left(q,\dot{q},-\hat{M}^{-1}\tau\right)\theta - \hat{M}\ddot{q} \\ &\quad - \left(-\tau + \hat{\Psi}_{rem}(q,\dot{q})\theta\right) - \hat{M}\ddot{q} = \qquad (23) \\ &\quad \tau - \hat{\Psi}(q,\dot{q},\ddot{q})\theta, \qquad (24) \end{aligned}$$

where $\hat{\Psi}_{rem}(q,\dot{q})$ means the remaining terms of $\hat{\Psi}$ function after removing the terms corresponding to $\ddot{q}$, viz. $\hat{M}\ddot{q}$ according to the definition in IV-A.2.

The final result gives an accurate transformation to the errors in the required coordinate, provided that the system follows the desired trajectory. In general, the feedback controller is assumed to insure that the system roughly follows the trajectory.

4) Prior and Posterior Probabilities: We introduced temporal continuity as a prior probability which overall contributes in reducing the chattering effect [14].

Additionally, we used the same transformation $\chi(e(t))$ for calculating the responsibility signals. This implies an assumption of a Gaussian error in the prediction of τ instead of $\ddot{q}$.

V. EXPERIMENTS AND RESULTS

In order to test the complete plant, a similar setup to [18] was considered. The task was following a star pattern in a workspace centered at $(15^\circ, 85^\circ)$ degrees. Each movement was supposed to be carried out along a path of 10 [cm] and last for 0.65 [s]. However, it was further allowed to settle in 0.65 [s] resulting in the total experiment time of 1.3 [s]. The delay from the sensory measurements was set to 30 [ms]. Two modules for each direction resulting in 16 modules were considered.

For the feedback controller representing joint stiffness and viscosity, the parameters were chosen in the actual measurement range specified by [24].

$$K_P = \begin{bmatrix} 15.00 & 6.15 \\ 6.00 & 15.40 \end{bmatrix}, \ K_D = \begin{bmatrix} 2.3 & 0.9 \\ 0.9 & 2.3 \end{bmatrix} \tag{25}$$

A translation invariant field in the workspace for the external field was considered:

$$f = B\dot{x}, \tag{26}$$

where f is a force vector, $\dot{x}$ the hand velocity vector, and B is a constant matrix representing viscosity of the environment in the end-point coordinates. We chose B to be

$$B = \begin{bmatrix} -2.525 & -2.8 \\ -2.8 & 2.775 \end{bmatrix} \ [\mathrm{Nsm}^{-1}]. \tag{27}$$

[1]e.g. note that all the functions built by invertible linear transforming of the coefficients are equivalent, since there is a one-to-one mapping between their θ:s.

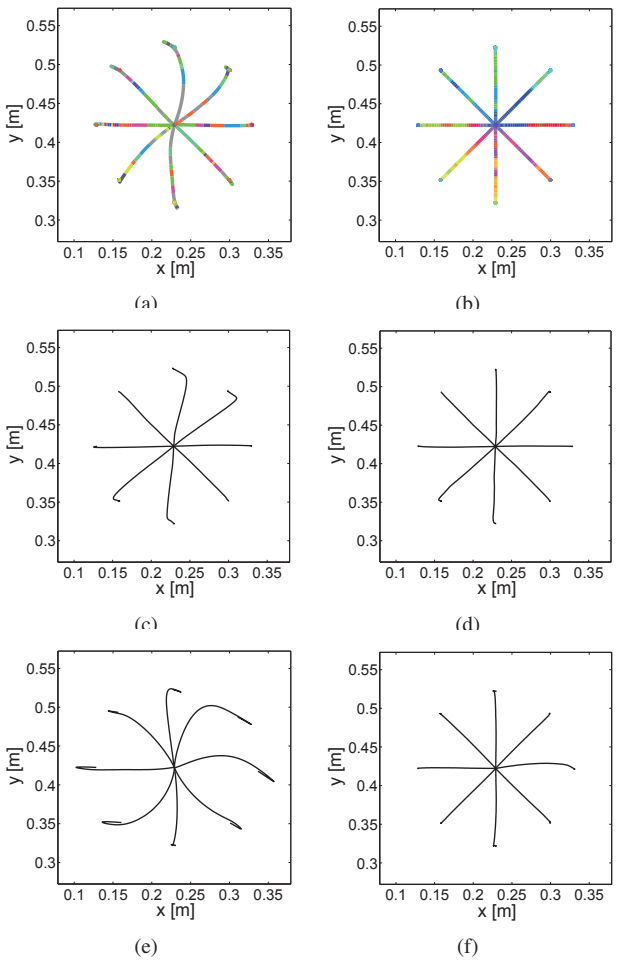

Fig. 3. Hand trajectory (a) in a null field with no adaptation; (b) after practicing, the color represents the contributing modules; (c) when exposed to the force field with only a feedback controller; (d) after practicing having the cerebellar controller activated; (e) carrying the object without adaptation; (f) with adaptation, starting from 0° and continuing clockwise.

The extra load is a rod shape object orthogonally attached to the 2nd link with $m = 2$ [Kg] and $l = 0.6$ [m].

The figures in this section show the performance of the cerebellar controller for different scenarios. We examined adaptation and generalization properties in a null field and in the external field. In addition, it was checked whether the system is capable of handling an unknown object.

From Fig. 4(a), and 4(b), it is clear that the cerebellar controller has correctly learned the nonlinearities of the arm and compensated for them by the feedforward signal. By color coding the modules, it is possible to visualize the contributing modules along the trajectory. Fig. 3(a) shows that before training many modules are activated simultaneously, hence the gray color, or the modules switch rapidly. On the contrary, Fig. 3(b) illustrates that after adaptation, the modules are activated in an orderly fashion.

According to Fig. 5, the parameters do not vary much across modules in a null field and reflect the physical parameters of the system. Whereas, the parameters related to the external field has distributed almost symmetrically with respect to the origin of the workspace.

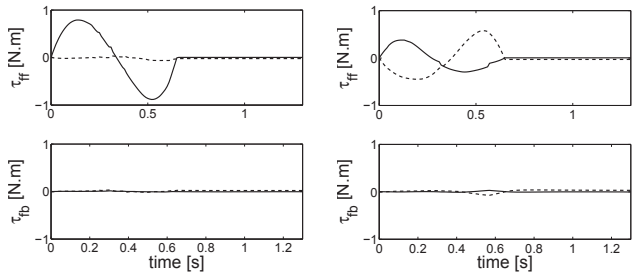

Fig. 4. Feedforward and feedback components of the control signal in 90° direction after practicing. The upper pane corresponds to the cerebellar controller output and the lower pane to the feedback controller. The solid and the dashed lines correspond to the first and the second joint, respectively.

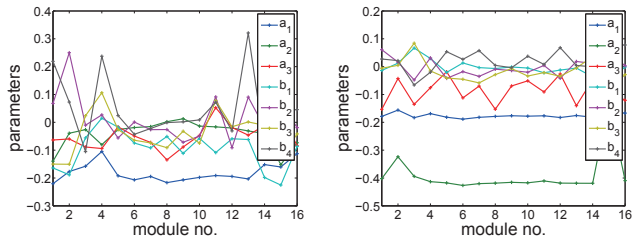

Fig. 5. Parameters across modules after training

VI. DISCUSSION

It is important to note that in ORF-MOSAIC neither the parameters of the dynamic equation nor the full structure of the functions are known to the controller. Nonetheless, the system manages to adapt in a few trials and overcome the "curse of dimensionality." We believe ORF-MOSAIC achieves this by efficiently combining different modules.

As the results show, there is a bigger variation in the field related parameters compared to the rest. It is due to the fact that in our parametrization, a constant force field in the joint space was considered whereas the experiments were done with a constant force field in the workspace. Since this force field varies with the joint angels, a controller with the same parametrization but a perfect knowledge of $\Psi(q,\dot{q},\ddot{q})$ would not be able to totally compensate for this. However, as it was expected, partitioning the subspace with different modules allowed each module to specialize in a region thus reducing the effect of the external field.

We have not investigated the stability of the system in the Lyapunov sense. It might be possible to combine the ideas from [25] with the approximate formulation of (18) to achieve this end. Although the goal of a control system could be summarized as trajectory following, the body might take into account an optimal strategy with respect to energy consumption or other criteria. Since tensing a muscle results in an increase in its metabolism, the minimization of the tensions across muscles follows the same principle. However, optimization with a more generic perspective would require considering the task as well. To address this, simultaneous treatment of adaptation and optimal control would be the

right approach [26], [27].

It is possible to draw a parallel between the modular structure proposed in this work and microzonal structure of the cerebellum [9]. Each module is adjusted in a certain arm configuration corresponding to certain cutaneous and proprioceptive inputs. The adjustment of parameters aims to make correction in the movement with respect to the desired trajectory. Hence, an error in the receptive field of an adjustment signal (corresponding to a climbing fiber) affects the activation of a set of muscles which would cancel it. This interpretation is in general agreement with the findings about the receptive fields in the cerebellar circuitry [28], [29].

VII. CONCLUSIONS AND FUTURE WORKS

In this paper, a novel cerebellar controller based on MOSAIC model [6] was proposed. We took inspiration from the microzonal structure of the cerebellum [9] as well as common control techniques to formulate this controller. A simplified model of a human arm including a muscular system were used as the test platform. To resolve the redundancy issue of the muscles, a minimum tension strategy was proposed which allows agile movements without excessive effort. Through simulations, it was shown that the system is able to adapt to the parameters of the arm, the external field and the changes in the load carried by the arm despite a moderate delay in the feedback signals received by this controller.

The new formulation offers interesting properties such as meaningful parameters compared to artificial neural networks. It has also an interesting implication for distributed control since each module only requires to know about the total contribution and not individual contributions hence makes little demand on sharing information among modules.

Finally based on the conceptual idea of ORF-MOSAIC, understanding the partitioning principle of microzones in terms of kinematic and dynamic variables could add a new perspective into understanding of the cerebellar control. Simulation of skin and proprioceptive receptors could be a key to this area.

REFERENCES

[1] J. S. Albus, "A New Approach to Manipulator Control: the Cerebellar Model Articulation Controller (CMAC)," *J. Dynamic Systems, Measurement, and Control*, vol. 97, pp. 220–227, 1975.

[2] J. C. Houk, J. T. Buckingham, and A. G. Barto, "Models of the cerebellum and motor learning," *Behavioral and Brain Sciences*, vol. 19, pp. 368–383, 1996.

[3] N. Schweighofer, J. Wolpert, Spoelstra, M. A. Arbib, and M. Kawato, "Role of the cerebellum in reaching movements in humans. II. A neural model of the intermediate cerebellum," *Eur. J. Neuroscience*, vol. 10, pp. 95–105, 1998.

[4] M. Kawato and H. Gomi, "The cerebellum and VOR/OKR learning models," *Trends in Neurosciences*, vol. 15, no. 11, pp. 445 – 453, 1992.

[5] D. M. Wolpert and M. Kawato, "Multiple paired forward and inverse models for motor control," *Neural Networks*, vol. 11, no. 7-8, pp. 1317 – 1329, 1998.

[6] M. Haruno, D. M. Wolpert, and M. M. Kawato, "MOSAIC Model for Sensorimotor Learning and Control," *Neural Comput.*, vol. 13, pp. 2201–2220, October 2001.

[7] D. M. Wolpert, R. C. Miall, and M. Kawato, "Internal models in the cerebellum," *Trends in Cognitive Sciences*, vol. 2, no. 9, pp. 338 – 347, 1998.

[8] F. A. Mussa-Ivaldi, "Modular features of motor control and learning," *Current Opinion in Neurobiology*, vol. 9, no. 6, pp. 713 – 717, 1999.

[9] M. Garwicz, C.-F. Ekerot, and H. Jörntell, "Organizational principles of cerebellar neuronal circuitry." *News Physiol. Sci.*, vol. 13, pp. 26–32, Feb 1998.

[10] M. Garwicz, H. Jörntell, and C. F. Ekerot, "Cutaneous receptive fields and topography of mossy fibres and climbing fibres projecting to cat cerebellar C3 zone." *J. Physiol.*, vol. 512 (Pt 1), pp. 277–293, Oct 1998.

[11] M. Haruno, D. M. Wolpert, and M. Kawato, "Multiple paired forward-inverse models for human motor learning and control," in *Proc. 1998 conf. on Advances in Neural Information Processing Systems II*. Cambridge, MA, USA: MIT Press, 1999, pp. 31–37.

[12] ——, "Hierarchical MOSAIC for movement generation," in *Excepta Medica International Coungress Series*, T. Ono, G. Matsumoto, R. Llinas, A. Berthoz, R. Norgren, H. Nishijo, and R. Tamura, Eds., vol. 1250. Amsterdam, The Netherlands: Elsevier Science B.V., 2003, pp. 575–590.

[13] N. Sugimoto, J. Morimoto, S.-H. Hyon, and M. Kawato, "eMOSAIC model for humanoid robot control," in *Proc. 11th int. conf. on Simulation of Adaptive Behavior: from animals to animats*, ser. SAB'10. Berlin, Heidelberg: Springer-Verlag, 2010, pp. 447–457.

[14] K. Doya, K. Samejima, K.-i. Katagiri, and M. Kawato, "Multiple model-based reinforcement learning." *Neural Comput.*, vol. 14, no. 6, pp. 1347 – 1369, 2002.

[15] M. Emadi Andani, F. Bahrami, and P. Jabehdar Maralani, "AMA-MOSAICI: An automatic module assigning hierarchical structure to control human motion based on movement decomposition," *Neurocomput.*, vol. 72, pp. 2310–2318, June 2009.

[16] T. Flash, "The control of hand equilibrium trajectories in multi-joint arm movements," *Biological Cybernetics*, vol. 57, pp. 257–274, 1987.

[17] N. Schweighofer, M. A. Arbib, and M. Kawato, "Role of the cerebellum in reaching movements in humans. I. Distributed inverse dynamics control." *Eur. J. Neuroscience*, vol. 10, no. 1, pp. 86–94, 1998.

[18] R. Shadmehr and O. A. Mussa-Ivaldi, "Adaptive representation of dynamics during learning of a motor task," *J. Neuroscience*, vol. 14, pp. 3208–3224, 1994.

[19] M. Kawato, "Internal models for motor control and trajectory planning," *Current Opinion in Neurobiology*, vol. 9, no. 6, pp. 718 – 727, 1999.

[20] M. Hulliger, "The mammalian muscle spindle and its central control," in *Reviews of Physiology, Biochemistry and Pharmacology, Volume 101*, ser. Ergebnisse der Physiologie Biologischen Chemie und Experimentellen Pharmakologie, K. Kramer, O. Krayer, E. Lehnartz, A. v. Muralt, and H. H. Weber, Eds. Springer Berlin Heidelberg, 1984, vol. 101, pp. 1–110.

[21] E. B. Benoni, "Cutaneous afferents provide information about knee joint movements in humans." *J. Physiology*, vol. 531, no. Pt 1, pp. 289–297, 2001.

[22] H. Hatze, "A mathematical model for the computational determination of parameter values of anthropomorphic segments," *J. Biomechanics*, vol. 13, no. 10, pp. 833 – 843, 1980.

[23] M. Katayama and M. Kawato, "Virtual trajectory and stiffness ellipse during multijoint arm movement predicted by neural inverse models," *Biological Cybernetics*, vol. 69, pp. 353–362, 1993.

[24] F. Mussa-Ivaldi, N. Hogan, and E. Bizzi, "Neural, mechanical, and geometric factors subserving arm posture in humans," *J. Neuroscience*, vol. 5, no. 10, pp. 2732–2743, 1985.

[25] R. Johansson, "Adaptive control of robot manipulator motion," *IEEE Trans. Robot. Autom.*, vol. 6, no. 4, pp. 483–490, 1990.

[26] ——, "Quadratic optimization of motion coordination and control," *IEEE Trans. Autom. Control*, vol. 35, no. 11, pp. 1197–1208, 1990.

[27] R. Johansson, P.-A. Fransson, and M. Magnusson, "Optimal coordination and control of posture and movements." *J. Physiol. Paris*, vol. 103, no. 3-5, pp. 159–177, 2009.

[28] R. Apps and M. Garwicz, "Anatomical and physiological foundations of cerebellar information processing." *Nat. Rev. Neurosci.*, vol. 6, no. 4, pp. 297 – 311, 2005.

[29] P. Dean, J. Porrill, C.-F. Ekerot, and H. Jörntell, "The cerebellar microcircuit as an adaptive filter: experimental and computational evidence." *Nat. Rev. Neurosci.*, vol. 11, no. 1, pp. 30–43, Jan 2010.